AGU PUBLICATIONS

Geophysical Research Letters

RESEARCH LETTER
10.1002/2015GL064623

Increase of the electric field in head-on collisions between negative and positive streamers

Mohand A. Ihaddadene[1] and Sebastien Celestin[1]

[1] Laboratory of Physics and Chemistry of the Environment and Space (LPC2E), University of Orleans, CNRS, Orleans, France

Key Points:
- Streamer collisions are not a source of significant X-ray emission
- The strong electric field produced collapses over an extremely short timescale
- Such collisions present an optical signature that can be looked for in observations

Supporting Information:
- Movie S1

Correspondence to:
M. A. Ihaddadene,
mohand.ihaddadene@cnrs-orleans.fr

Citation:
Ihaddadene, M. A., and S. Celestin (2015), Increase of the electric field in head-on collisions between negative and positive streamers, *Geophys. Res. Lett.*, *42*, 5644–5651, doi:10.1002/2015GL064623.

Received 20 MAY 2015
Accepted 16 JUN 2015
Accepted article online 18 JUN 2015
Published online 14 JUL 2015

Abstract Head-on collisions between negative and positive streamer discharges have recently been suggested to be responsible for the production of high electric fields leading to X-rays emissions. Using a plasma fluid approach, we model head-on collisions between negative and positive streamers. We observe the occurrence of a very strong electric field at the location of the streamer collision. However, the enhancement of the field produces a strong increase in the electron density, which leads to a collapse of the field over only a few picoseconds. Using a Monte Carlo model, we have verified that this process is therefore not responsible for the acceleration of a significant number of electrons to energy >1 keV. We conclude that no significant X-ray emission could be produced by the head-on encounter of nonthermal streamer discharges. Moreover, we quantify the optical emissions produced in the streamer collision.

1. Introduction

The processes responsible for the production of high-energy radiation in thunderstorms and laboratory discharges are not fully understood yet. X-ray bursts have been detected from the ground during the descent of natural negative lightning stepped leader [*Moore et al.*, 2001] and rocket-triggered lightning flashes [*Dwyer et al.*, 2003]. Recently, observational studies have been dedicated to understand these emissions in lightning [e.g., *Howard et al.*, 2008; *Saleh et al.*, 2009; *Dwyer et al.*, 2011; *Schaal et al.*, 2014], and laboratory experiments have confirmed that atmospheric pressure discharges produce X-rays [e.g., *Dwyer et al.*, 2005; *Rahman et al.*, 2008; *Nguyen et al.*, 2008, 2010; *March and Montanyà*, 2011; *Kochkin et al.*, 2012, 2015].

The emission of X-rays by lightning discharges is believed to be caused by the production of thermal runaway electrons [*Dwyer*, 2004]. Indeed, *Moss et al.* [2006] have suggested that the strong electric fields that are produced in streamer heads could be responsible for thermal runaway electron production and *Celestin and Pasko* [2011] have shown how large fluxes of runaway electrons could be produced by streamer discharges propagating under strong electric fields such as those present at the leader tip. Recently, *Babich et al.* [2015]) have suggested that thermal runaway electrons could be produced by streamer discharges guided by precursor streamer channels. Moreover, it is interesting to note that based on the theory of production of thermal runaway electrons by streamers at the leader front, *Xu et al.* [2014] have shown that negative leaders forming potential drops of approximately 5 MV in their tip region would produce X-ray spectra similar to observational results of *Schaal et al.* [2012] in terms of general shape and spectral hardness.

Encounters between streamers of opposite polarities are believed to be very common in nature and laboratory experiments. In particular, during the formation of a new leader step, the negative streamer zone around the tip of a negative leader and the positive streamers initiated from the positive part of a bidirectional space leader strongly interact and numerous head-on encounters are expected. In laboratory experiments, when streamers are approaching a sharp electrode, streamer discharges with the opposite polarity are initiated from this electrode and collide with the approaching streamers. *Cooray et al.* [2009] suggested that head-on collisions between negative and positive streamers could produce extremely strong electric fields that would lead to the production of thermal runaway electrons and corresponding X-rays. On the basis of experimental evidence, *Kochkin et al.* [2012] recently concluded that X-ray bursts over a timescale shorter than a few nanoseconds were indeed produced by collisions between positive and negative streamers, but X-ray detections could not be related to specific streamer collisions [see also *Kochkin et al.*, 2015, section 3.5.2].

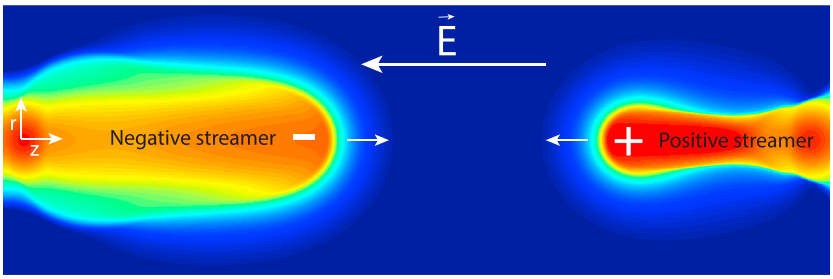

Figure 1. Illustration of a head-on collision between a positive (right) and a negative streamer (left) moving toward each other under an external electric field $\vec{E}$.

However, the estimation of the increase in the electric field during encounters of streamers with opposite polarities (see Figure 1) is a complicated problem. Indeed, an increase of the field beyond the conventional breakdown threshold would rapidly increase the electron density at the location of the encounter. In turn, one expects that the field would swiftly collapse due to the corresponding increase in the electron density.

In this paper, we investigate this nonlinear problem using a nonthermal plasma fluid model and estimate upper limits on fluxes of high-energy electrons and photons possibly produced in this process using Monte Carlo simulations.

2. Model Formulation

The streamer model we use in the present study is based on the drift-diffusion equations for charged species. These equations are numerically solved using the finite volume methods in cylindrically symmetric geometry. The drift-diffusion equations are coupled with Poisson's equation as follows:

$$\frac{\partial n_e}{\partial t} + \nabla \cdot n_e \vec{v}_e - D_e \nabla^2 n_e = S_{ph} + S_e^+ - S_e^- \tag{1}$$

$$\frac{\partial n_p}{\partial t} = S_{ph} + S_p^+ \tag{2}$$

$$\frac{\partial n_n}{\partial t} = S_n^+ \tag{3}$$

$$\nabla^2 \phi = -\frac{q}{\varepsilon_0}(n_p - n_n - n_e) \tag{4}$$

where subscripts "e," "p," and "n" refer to electrons, positive ions, and negative ions, respectively; n_i is the number density of species i; v_e is the electron drift velocity; and D_e, q, ε_0, and ϕ are the electron diffusion coefficient, the absolute value of the electron charge, the permittivity of free space, and the electric potential, respectively. Over the time scale of interest here, ions are considered to be motionless. The S^+ and S^- terms stand for the rates of production by electron impact ionization and loss of electrons by attachment, respectively. The transport coefficients and source terms S^+ and S^- are defined using analytical formulas defined in the appendix of *Morrow and Lowke* [1997]. The S_{ph} term defines the rate of production of electron positive-ion pairs caused by the photoionization process [*Zheleznyak et al.*, 1982; *Liu and Pasko*, 2004].

To solve numerically equations (1)–(4), we use the finite volume methods coupled with a flux-corrected transport (FCT) technique for steep gradients developed by *Zalesak* [1979]. An upwind scheme and a fourth-order finite difference scheme have been used to calculate the low- and high-order fluxes required in the FCT, respectively [see *Zalesak*, 1979, Appendix]. To avoid spurious oscillations that appear near the axis of symmetry in the region of the streamer head where steep density and electric field gradients are significant, we use a logarithmic function to calculate the fourth-order finite difference scheme to which we add fourth-order dissipative fluxes [see *Kuzmin et al.*, 2012, pp. 23–65] in order to damp the spurious amplifications of the electron density caused by the FCT technique. The finite difference form of Poisson's equation is solved using

a successive over-relaxation (SOR) method that we have developed. The boundary conditions applied to Poisson's equation are the following: $\frac{\partial\phi}{\partial r}|_{r=0} = 0$, $\phi(0 \le r \le 1.92\ \text{mm}, z = 0) = 0$, $\phi\ (r, z = 8\ \text{mm}) = U$, and $\phi\ (r = 1.92\ \text{mm}, 0 \le z \le 8\ \text{mm}) = U\times$ (z/8 mm), where $U = 32$ kV or 48 kV and corresponds to amplitudes of homogeneous Laplacian fields $E_0 = 40$ kV/cm and $E_0 = 60$ kV/cm, respectively, between the plane electrodes.

Positive and negative streamers are initiated on each side of the simulation domain by placing two Gaussians of neutral plasma with characteristic sizes $\sigma_z = 200$ μm and $\sigma_r = 200$ μm in the vicinity of each electrode.

The photoionization term is evaluated using an integral approach [*Zheleznyak et al.*, 1982; *Liu and Pasko*, 2004] in cylindrical coordinates. In a region around the maximum of the photoionization source, the term S_{ph} is estimated at every grid points. In other regions, one point over 10 is estimated, and a linear interpolation technique is employed. We have verified that this technique gives very similar results as those obtained through more sophisticated methods [see *Bourdon et al.*, 2007].

We quantify the density of excited species of $N_2(B^3\Pi_g)$, $N_2(C^3\Pi_u)$, and $N_2^+(B^2\Sigma_u^+)$ associated with optical emissions of the first positive band system of N_2 ($1PN_2$), the second positive band system of N_2 ($2PN_2$), and the first negative band system of N_2^+ ($1NN_2^+$), respectively. As in the study reported by *Xu et al.* [2015] quenching of $N_2(B^3\Pi_g)$ and $N_2(C^3\Pi_u)$ is considered to occur through collisions with N_2 and O_2 with rate coefficients $\alpha_1 = 10^{-11}$ cm^3/s [*Kossyi et al.*, 1992] and $\alpha_2 = 3 \times 10^{-10}$ cm^3/s [*Vallance Jones*, 1974, p. 119], respectively. $N_2(B^2\Sigma_u^+)$ is quenched by N_2 with a rate coefficient $\alpha_1 = 4.53 \times 10^{-10}$ cm^3/s and by O_2 with a rate coefficient $\alpha_2 = 7.36 \times 10^{-10}$cm^3/s [e.g., *Mitchell*, 1970; *Pancheshnyi et al.*, 1998; *Kuo et al.*, 2005].

The density of excited species is estimated according to the following differential equation [*Liu and Pasko*, 2004]:

$$\frac{\partial n_k}{\partial t} = -\frac{n_k}{\tau_k} + \nu_k n_e + \sum_m n_m A_m \tag{5}$$

where $\tau_k = [A_k + \alpha_1 N_{N_2} + \alpha_2 N_{O_2}]^{-1}$ and A_k are the characteristic life time and Einstein's coefficient of the excited species k. The quantities n_k and ν_k are, respectively, the density and the excitation frequency of the excited species k. The sum over $n_m A_m$ takes into account the cascading of excited species from higher energy levels m to the level k.

Moreover, the associated optical emissions are evaluated according to the following integral along the line of sight [*Liu and Pasko*, 2004]:

$$I_k = 10^{-6} \int_L A_k n_k \mathrm{d}l \tag{6}$$

where I_k and n_k are the intensity of optical emissions in Rayleighs and the number density of excited species k, respectively.

In this paper, we show simulation results performed at the ground-level air density $N = 2.688 \times 10^{25}$ m^{-3} under strong externally applied homogeneous electric fields with a spatial resolution $\Delta r = 8$ μm and $\Delta z = 8$ μm in a simulation domain (1001×241) discretized over regular grid points.

3. Results

3.1. Case $E_0 = 40$ kV/cm

As depicted in Figure 2a that shows the electric field along the z axis, one sees the positive streamer forming and propagating leftward as the negative streamer initiates and propagates rightward. The electric field in both negative and positive streamers reaches a stable value, before starting to rise when streamers start influencing each other. The local electric field strongly increases at the moment of the encounter between both streamer heads. We can clearly see the collapse of the electric field just after reaching a maximum (see Movie S1 in the supporting information) while a significant rise in the electron density is produced at the same location as shown in Figure 2c. Figure 2d (solid line) shows the behavior of the maximum electric field in the simulation domain as function of time for the case of an externally applied homogeneous electric field $E_0 = 40$ kV/cm. The maximum electric field in the simulation domain reaches 235 kV/cm, which is lower than the thermal runaway threshold as defined by the maximum electron friction force around ~100 eV (~260 kV/cm under ground-level air density). Once the electric field in the streamer heads is stable, the average velocity before collision is estimated to be ~10^6 m/s.

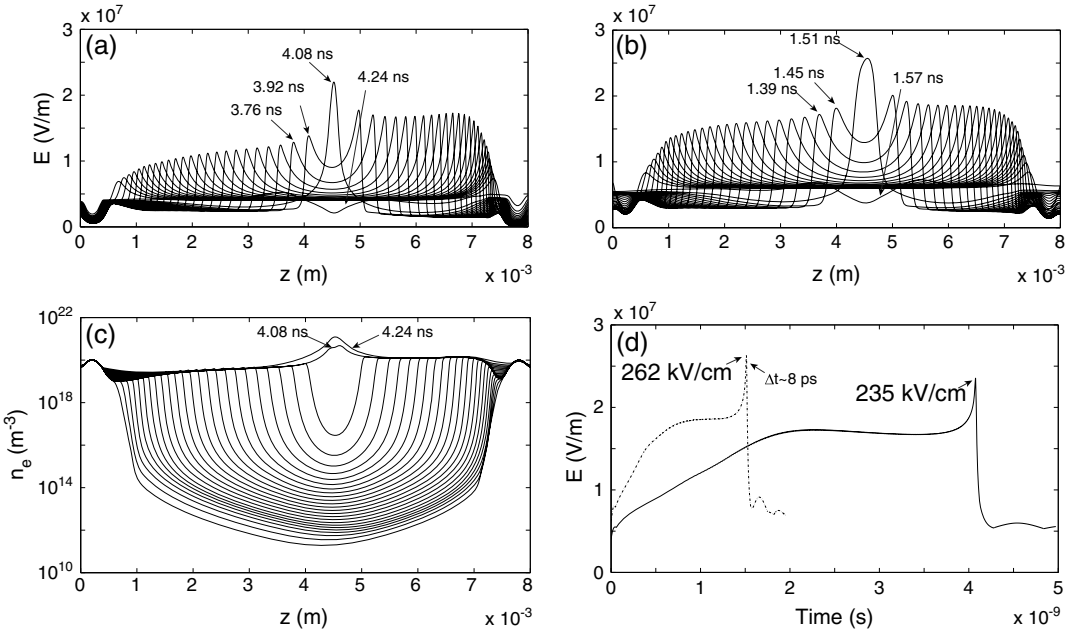

Figure 2. (a and b) Profile of the electric field along the *z* axis in the case $E_0 = 40$ kV/cm and 60 kV/cm, respectively. (c) Profile of the electron density along the *z* axis in the case $E_0 = 40$ kV/cm. (d) Evolution of the maximum electric field E_{max} as a function of time. Solid and dashed lines correspond to the cases $E_0 = 40$ and 60 kV/cm, respectively. In Figures 2a and 2c, results are shown with a time step of 160 ps. In Figure 2b, results are shown with a time step of 60 ps.

3.2. Case $E_0 = 60$ kV/cm

Figure 2d (dashed line) shows the behavior of the maximum electric field in the simulation domain as function of time and (Figure 2b) the electric field along the *z* axis for the case $E_0 = 60$ kV/cm. We observe a similar behavior of the electric field as in the case $E_0 = 40$ kV/cm; however, the maximum value reached is 262 kV/cm. After reaching a maximum of 262 kV/cm, the electric field collapses over a very short duration of ~4 ps. The total time over which the electric field is greater than 250 kV/cm is approximately ~8 ps. The maximum electric field reached is greater than that obtained in the situation where the homogeneous electric field is $E_0 = 40$ kV/cm and the average velocity of streamers before the encounter is greater as well ($\sim 3 \times 10^6$ m/s).

3.3. Estimate of the Number of High-Energy Electrons and Photons Produced During the Encounter of Streamers With Opposite Polarities

Very high amplitudes of the electric field are obtained in both cases described above. In order to quantify the fluxes of high-energy electrons and the corresponding bremsstrahlung photons produced during the streamers collision, we have used a Monte Carlo code that simulates the propagation of electrons in air with energies from sub-eV to MeVs under externally applied electric fields (see *Celestin and Pasko* [2011] for more details) in a two-step fashion. In the first step, we calculate the electric field during the streamer collision through our plasma fluid model as described above. In the second step, we follow the dynamics of test electrons initiated with an energy of 1 eV and distributed over space using our Monte Carlo code under the electric fields varying in space and time that were obtained in the first step. The number of electrons needed in this configuration has proven computationally impractical on ~100 processors to obtain an accurate estimate on the production of high-energy electrons. For the sake of simplicity, we therefore estimate an upper limit of the flux of high-energy electrons by using a time-varying homogeneous electric field equal to the maximum field obtained in our streamer simulation domain at each moment of time as shown in Figure 2d. We emphasize that this method strongly overestimates the number and energy of electrons obtained since electric field gradients are neglected.

In the case of an applied field of $E_0 = 60$ kV/cm, at the moment of the collision the conduction current at the position of the peak electric field (see Figure 2b) reaches 20 A. For comparison, the conduction current evaluated locally in the positive streamer head when the electric field has reached a stable amplitude ($t \simeq 1$ ns, see Figure 2d) is ~15 A, which is consistent with the amplitude of conduction current in a streamer head reported in the literature [e.g., *Liu*, 2010], considering that the external electric field applied in the present

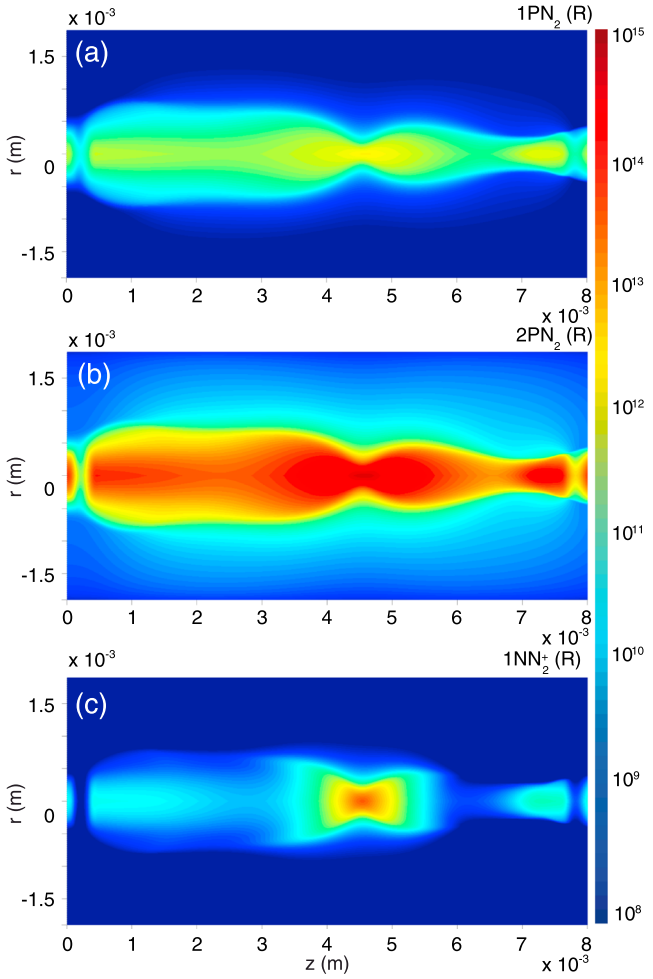

Figure 3. (a–c) Optical emissions $1PN_2$, $2PN_2$, and $1NN_2^+$ 30 ps after the head-on collision in the case of $E_0 = 40$ kV/cm.

study is very strong (see section 4). From this maximum current, one can directly estimate the total number of electrons passing through a surface perpendicular to the streamer axis per unit time during the streamer collision. Additionally, our Monte Carlo simulation results indicate that, in the case of $E_0 = 60$ kV/cm, the ratio between electrons with energies greater than 1 keV to the total number of electrons is lower than 1.5×10^{-7}. During the streamer collision, the strong increase in the electric field takes place over a duration shorter than 0.1 ns (see Figure 2d). Hence, one can estimate that during this time, an upper limit of $20/q_e \times 1.5 \times 10^{-7} \times 0.1 \times 10^{-9} \simeq 2000$ electrons with energy greater than 1 keV could be produced.

3.4. Associated Optical Emissions

Figures 3a–3c show the associated optical emissions for $1PN_2$, $2PN_2$, and $1NN_2^+$ band systems. The maximum peaks of the density of the excited species and corresponding optical emissions are obtained after the maximum electric field was reached. In Figure 3, the results correspond to a time ~30 ps after the collision. We clearly see that the luminosity increases in the zone of the collision, which could be used as a signature of head-on encounters between positive and negative streamers.

4. Discussion

A very high maximum electric field of 262 kV/cm has been obtained locally during the head-on collision of negative and positive streamers propagating under a homogeneous electric field of 60 kV/cm. After a series of tests performed using a Monte Carlo model in which we have introduced the electric field obtained in our streamer simulations, we have found that only a maximum of 2000 electrons with energy > 1 keV could

be produced by the encounter of streamers with opposite polarities studied in this paper due to the rapid collapse of the strong field produced during the streamer collision (see Figure 2d). This estimate is done in the case of E_0 = 60 kV/cm and would be lower in the case of a weaker applied field since the resulting maximum field reached during the streamers collision would be weaker as well (see Figure 2d). In order to estimate the number of bremsstrahlung X-rays produced by these electrons, one can use the Bethe-Heitler differential cross section [e.g., *Lehtinen*, 2000, pp. 45–49]. We find that the frequency of X-ray production with energy greater than 1 keV by electrons with energy of a few keVs in air at ground level is on the order of $\sim 10^5$ s^{-1}. For comparison, using the same cross section and air density, an electron with an energy of 1 MeV is associated with an X-ray (> 1 keV) production frequency of $\sim 6 \times 10^6$ s^{-1}. In our simulation results, electrons with energy greater than 1 keV are only present for a very short time on the order of a few picoseconds. Assuming that these electrons could be present over a timescale corresponding to the timescale of the whole increase of the electric field (~0.1 ns), one finds that only $10^5 \times 2000 \times 0.1 \times 10^{-9} \simeq 0.02$ X-rays with energy greater than 1 keV would be produced per streamers encounter.

If one considers that, once produced, energetic electrons could still accelerate in the electrode gap [*Cooray et al.*, 2009], a longer X-ray emission timescale should be considered. Experiments of spark discharges producing X-rays usually involve electrode gaps of ~1 m [e.g., *Dwyer et al.*, 2008; *Kochkin et al.*, 2012]. An electron with an energy of 1 keV has a velocity of $\sim 2 \times 10^7$ m/s, corresponding to a propagation lasting 50 ns over 1 m. Hence, one estimates an upper limit of 10 X-rays with energy >1 keV produced by the propagation of such 2000 electrons over the whole electrode gap. We emphasize that physical parameters have been maximized to obtain this upper limit. Given the very low number of X-rays obtained through the mechanism of encounters of streamers with opposite polarities, it is unlikely that these photons could be detected.

The electric field at the streamer head is partly controlled by the externally applied Laplacian electric field. The reason why we have used very strong externally applied ambient fields of 40 and 60 kV/cm is to increase the electric field at the heads of both streamers to maximize the probability of producing thermal runaway electrons. This had an impact on the velocity of streamers as well. As obvious in Figure 2d, the collision corresponding to E_0 = 60 kV/cm occurred earlier in time than that of E_0 = 40 kV/cm. We emphasize that the homogeneous fields used in this paper are much stronger than fields usually present in the middle of 1 m spark gaps.

It is important to note that the significant amount of excited species produced during the head-on encounter of streamers and the associated optical emissions can be used as a signature to determine if a collision between streamers of opposite polarity actually took place.

The head-on collision patch of the optical emission is reminiscent of luminous patches observed in sprites and named sprite beads [e.g., *Cummer et al.*, 2006; *Stenbaek-Nielsen and McHarg*, 2008; *Luque and Gordillo-Vasquesz*, 2011]. Note that *Cummer et al.* [2006] had already found out that collisions between downward streamers and adjacent streamer channels form long-lasting sprite beads. However, the duration of the luminous patch found in our simulations is too short to account for durations up to 1 s, even if scaled to high altitude. Indeed, we have performed similar simulations as those presented in the present paper with an air density corresponding to 70 km altitude and found that the luminous patch lasts over a few microseconds for $2PN_2$ and $1NN_2^+$ and ~10 μs for $1PN_2$. Nevertheless, other physical processes such as chemical reactions unaccounted for in the present study or long-lasting continuing current of the sprite producing lightning discharge may have a significant effect on the overall duration of these luminous patches and sprite produced by inhomogeneities placed at different altitudes may encounter and produce associated optical patches similar to those reported in the present study.

5. Conclusions

The main conclusions of this work can be summarized as follows:

1. We have simulated the head-on collision between positive and negative streamers and have showed that this process is not likely to produce significant number of thermal runaway electrons with energy >1 keV and the corresponding X-rays.
2. Despite the very high peak electric field obtained during the streamer collision, the corresponding rapid collapse of the electric field over a few picoseconds due to the large increase of the conductivity at the same location prevents efficient production of thermal runaway electrons.

3. We have quantified the amount of excited species and the associated optical emissions. We show that the occurrence of the streamer collision is followed by a peak of optical emissions associated with $1PN_2$, $2PN_2$, and $1NN_2^+$ band systems (luminous patch). This may be used as a signature of streamer head-on collisions and corresponding experimental verification of the capability of streamer collisions to produce X-rays.

Acknowledgments
This work is supported by the French space agency (CNES) as part of TARANIS space mission and by the French Region Centre-Val de Loire. Results of Monte Carlo simulation presented in this paper have been obtained using the computer cluster at the Centre de Calcul Scientifique en Région Centre-Val de Loire (CCSC). All data used in this paper are directly available after a request is made to authors M.A.I. (mohand.ihaddadene@cnrs-orleans.fr) or S.C. (sebastien.celestin@cnrs-orleans.fr).

The editor thanks Meagan Schaal and an anonymous reviewer for assistance evaluating this manuscript.

References

Babich, L. P., E. I. Bochkov, I. M. Kutsyk, T. Neubert and O. Chanrion (2015), A model for electric field enhancement in lightning leader tips to levels allowing X-ray and γ ray emissions, *J. Geophys. Res. Space Physics*, *120*, doi:10.1002/2014JA020923, in press.

Bourdon, A., V. P. Pasko, N. Y. Liu, S. Célestin, P. Ségur, and E. Marode (2007), Efficient models for photoionization produced by non-thermal gas discharges in air based on radiative transfer and the Helmholtz equations, *Plasma Sources Sci. Technol.*, *16*, 656–678, doi:10.1088/0963-0252/16/3/026.

Celestin, S., and V. P. Pasko (2011), Energy and fluxes of thermal runaway electrons produced by exponential growth of streamers during the stepping of lightning leaders and in transient luminous events, *Geophys. Res. Lett*, *116*, A03315, doi:10.1029/2010JA016260.

Cooray, V., L. Arevalo, M. Rahman, J. Dwyer, and H. Rassoul (2009), On the possible origin of X-rays in long laboratory sparks, *J. Atmos. Sol. Terr. Phys.*, *71*, 1890–1898, doi:10.1016/j.jastp.2009.07.010.

Cummer, S. A., N. Jaugey, J. Li, W. A. Lyons, T. E. Nelson, and E. A. Gerken (2006), Submillisecond imaging of sprite development and structure, *Geophys. Res. Lett.*, *33*, L04104, doi:10.1029/2005GL024969.

Dwyer, J. R. (2004), Implications of X-ray emission from lightning, *Geophys. Res. Lett*, *31*, L12102, doi:10.1029/2004GL019795.

Dwyer, J. R., et al. (2003), Energetic radiation produced during rocket-triggered lightning, *Science*, *299*, 694–697, doi:10.1126/science.1078940.

Dwyer, J. R., H. K. Rassoul, Z. Saleh, M. A. Uman, J. Jerauld, and J. A. Plumer (2005), X-ray bursts produced by laboratory sparks in air, *Geophys. Res. Lett.*, *32*, L20809, doi:10.1029/2005GL024027.

Dwyer, J. R., Z. saleh, H. K. Rassoul, D. Concha, M. Rahman, V. Corray, J. Jerauld, M. A. Uman, and V. A. Rakov (2008), A study of X-ray emission from laboratory sparks in air at atmospheric pressure, *J. Geophys. Res.*, *113*, D23207, doi:10.1029/2008JD010315.

Dwyer, J. R., M. Schaal, H. K. Rassoul, M. A. Uman, D. M. Jordan, and D. Hill (2011), High-speed X-ray images of triggered lightning dart leaders, *J. Geophys. Res.*, *116*, D20208, doi:10.1029/2011JD015973.

Howard, J., M. A. Uman, J. R. Dwyer, D. Hill, C. Biagi, Z. Saleh, J. Jerauld, and H. K. Rassoul (2008), Co-location of lightning leader X-ray and electric field change sources, *Geophys. Res. Lett.*, *35*, L13817, doi:10.1029/2008GL034134.

Kochkin, P. O., C. V. Nguyen, A. P. J. van Deursen, and U. Ebert (2012), Experimental study of hard X-rays emitted from metre-scale positive discharges in air, *J. Phys. D: Appl. Phys.*, *45*, 425202, doi:10.1088/0022-3727/45/42/425202.

Kochkin, P. O., A. P. J. van Deursen, and U. Ebert (2015), Experimental study on hard X-rays emitted from metre-scale negative discharges in air, *J. Phys. D: Appl. Phys.*, *48*(2), 025205, doi:10.1088/0022-3727/48/2/025205.

Kossyi, I. A., A. Y. Kostinsky, A. A. Matveyev, and V. P. Silakov (1992), Kinetic scheme of the non-equilibrium discharge in nitrogen-oxygen mixtures, *Plasma Sources Sci. Technol.*, *1*, 207–220, doi:10.1088/0963-0252/1/3/011.

Kuo, C.-L., R. R. Hsu, A. B. Chen, H. T. Su, L. C. Lee, S. B. Mende, H. U. Frey, H. Fukunishi, and Y. Takahashi (2005), Electric fields and electron energies inferred from the ISUAL recorded sprites,*Geophy. Res. Lett.*, *32*, L19103, doi:10.1029/2005GL023389.

Kuzmin, D., R. Löhner, and S. Turek (2012), *Flux-Corrected Transport*,Springer, Netherlands, doi:10.1007/978-94-007-4038-9.

Lehtinen, N. G. (2000), Relativistic runaway electrons above thunderstorms, PhD thesis, Standford Univ., Stanford, Calif.

Liu, N. (2010), Model of sprite luminous trail caused by increasing streamer current, *Geophy. Res. Lett.*, *37*, L04102, doi:10.1029/2009GL042214.

Liu, N., and V. P. Pasko (2004), Effects of photoionization on propagation and branching of positive and negative streamers in sprites, *J. Geophy. Res.*, *109*, A04301, doi:10.1029/2003JA010064.

Luque, A., and F. J. Gordillo-Vasquesz (2011), Sprite beads originating from inhomogeneities in the mesospheric electron density, *Geophy. Res. Lett.*, *38*, L04808, doi:10.1029/2010GL046403.

March, V., and J. Montanyà (2011), X-rays from laboratory sparks in air: The role of the cathode in the production of runaway electrons, *Geophys. Res. Lett.*, *38*, L04803, doi:10.1029/2010GL046540.

Mitchell, K. B. (1970), Fluorescence efficiencies and collisional deactivation rates for N_2 and N_2^+ bands excited by soft X-rays, *J. Chem. Phys.*, *53*, 1795–1802, doi:10.1063/1.1674257.

Moore, C. B., K. B. Eack, G. D. Aulich, and W. Rison (2001), Energetic radiation associated with lightning stepped-leaders, *Geophys. Res. Lett.*, *28*, 2141–2144.

Morrow, R., and J. J. Lowke (1997), Streamer propagation in air, *J. Phys. D: Appl. Phys.*, *30*, 614–627, doi:10.1088/0022-3727/30/4/017.

Moss, G. D., V. P. Pasko, N. Liu, and G. Veronis (2006), Monte Carlo model for analysis of thermal runaway electrons in streamer tips in transient luminous events and streamer zones of lightning leaders, *J. Geophys. Res.*, *111*, A02307, doi:10.1029/2005JA011350.

Nguyen, C. V., A. P. J. van Deursen, and U. Ebert (2008), Multiple X-ray bursts from long discharges in air, *J. Phys. D: Appl. Phys.*, *41*(23), 234012, doi:10.1088/0022-3727/41/23/234012.

Nguyen, C. V., A. P. J. van Deursen, E. J. M. van Heesch, G. J. J. Winands, and A. J. M. Pemen (2010), X-ray emission in streamer-corona plasma, *J. Phys. D: Appl. Phys.*, *43*(2), 025202, doi:10.1088/0022-3727/43/2/025202.

Pancheshnyi, S. V., S. M. Starikovskaia, and A. Y. Starikovskii (1998), Measurements of rate constants of the $N_2(C^3\Pi_u, v'=0)$ and $N_2^+(B^2\Sigma_u^+, v'=0)$ deactivation by N_2, O_2, H_2, CO and H_2O molecules in afterglow of the nanosecond discharge, *Chem. Phys. Lett.*, *294*, 523–527, doi:10.1016/S0009-2614(98)00879-3.

Rahman, M., V. Cooray, N. Azlinda Ahmad, J. Nyberg, V. A. Rakov, and S. Sharma (2008), X-rays from 80-cm long sparks in air, *Geophys. Res. Lett.*, *35*, L06805, doi:10.1029/2007GL032678.

Saleh, Z., J. Dwyer, J. Howard, M. Uman, M. Bakhtiari, D. Concha, M. Stapleton, D. Hill, C. Biagi, and H. Rassoul (2009), Properties of the X-ray emission from rocket-triggered lightning as measured by the Thunderstorm Energetic Radiation Array (TERA), *J. Geophys. Res.*, *114*, D17210, doi:10.1029/2008JD011618.

Schaal, M. M., J. R. Dwyer, Z. H. Saleh, H. K. Rassoul, J. D. Hill, D. M. Jordan, and M. A. Uman (2012), Spatial and energy distributions of X-ray emissions from leaders in natural and rocket triggered lightning, *J. Geophys. Res.*, *117*, D15201, doi:10.1029/2012JD017897.

Schaal, M. M., et al. (2014), The structure of X-ray emissions from triggered lightning leaders measured by a pinhole-type X-ray camera, *J. Geophys. Res.*, *119*, 982–1002, doi:10.1002/2013JD020266.

Stenbaek-Nielsen, H. C., and M. G. McHarg (2008), High time-resolution sprite imaging: Observations and implications, *J. Phys. D: Appl. Phys.*, *41*(23), 234009, doi:10.1088/0022-3727/41/23/234009.

Vallance Jones, A. V. (1974), *Aurora*, D. Reidel, Norwell, Mass.
Xu, W., S. Celestin, and V. P. Pasko (2014), Modeling of X-ray emissions produced by stepping lightning leaders, *Geophys. Res. Lett.*, *41*, 7406–7412, doi:10.1002/2014GL061163.
Xu, W., S. Celestin, and V. P. Pasko (2015), Optical emissions associated with terrestrial gamma ray flashes, *J. Geophys. Res. Space Physics*, *120*, 1355–1370, doi:10.1002/2014JA020425.
Zalesak, S. T. (1979), Fully multidimensional flux-corrected transport algorithms for fluids, *J. Comput. Phys.*, *31*, 335–362, doi:10.1016/0021-9991(79)90051-2.
Zheleznyak, M. B., A. K. Mnatsakanian, and S. V. Sizykh (1982), Photoionization of nitrogen and oxygen mixtures by radiation from a gas discharge, *High Temp.*, *20*, 357–362.